

Size Scaling of Third-Order Off-Resonant Polarizabilities. Electronic Coherence in Organic Oligomers

Michael Schulz, Sergei Tretiak, Vladimir Chernyak, and Shaul Mukamel*

Contribution from the Rochester Theory Center for Optical Science and Engineering and Department of Chemistry, University of Rochester P. O. RC Box 270216, Rochester, New York 14627-0216

Received April 5, 1999. Revised Manuscript Received September 24, 1999

Abstract: The variation of the nonlinear optical electronic polarizabilities of eight families of organic oligomers with molecular chain length is investigated using the coupled electronic oscillator (CEO) approach. Comparison of the saturation curves with contour plots of the first- and third-order density-matrix response shows a strong correlation between the magnitude of the saturation size, L_s , and the antidiagonal size of the density matrix, L_ρ , which constitutes a characteristic exciton size responsible for optical coherence. For the majority of oligomers investigated, L_s is linearly related to L_ρ .

1. Introduction

Materials with high optical nonlinearities are essential in the development of new information technologies and optical switching. Organic materials are of particular interest because of their high structural variability, high cost-effectiveness, low dielectric constants, fast nonlinear optical response, and high off-resonance nonlinear susceptibilities.^{1–3} Identifying the relation between optical nonlinearities and molecular structure is the key for a rational design of new nonlinear organic materials.^{1,4,5} The variation of optical polarizabilities in organic polymers with chain length has been the subject of numerous theoretical^{6–10} and experimental^{5,11} investigations.

In this paper we compute the linear and the third-order response of several families of conjugated organic oligomers using the collective electronic oscillator (CEO) approach.^{12,13} The nonlinear optical polarizabilities are interpreted using a real

space analysis, which provides a highly intuitive picture of the optical response.

The linear and nonlinear static response of organic molecules can be computed by solving the time-dependent Schrödinger equation for the many-electron wave function $\Psi(t)$. This may be accomplished using a variational/perturbative treatment of the ground state in the presence of the external electric field. The resulting Coupled-Perturbed Hartree-Fock (CPHF) procedure requires significantly larger basis sets and much more costly ab initio calculations than conventional Hartree-Fock computation of ground-state properties.² The configuration-interaction/sum-over-states (CI/SOS) method^{1,3} is a different widely used approach. The calculation of the optical response involves the computation of the ground-state and the excited-state wave functions as well as the dipole matrix elements.^{14,15} Even though the SOS method has a number of advantages, it is not necessarily size-consistent.^{16,17} Its convergence involves a delicate cancellation of very large positive and negative terms, which complicates its numerical implementation.

A major goal of these studies is to understand how the structures of complex molecules such as organic oligomers with a delocalized π -electronic system of the type shown in Figure 1 are related to their optical properties and how specific variations in molecular design, such as chain length or donor/acceptor substitutions, can impact the off-resonant infrared linear and nonlinear optical response. Both CPHF and SOS/CI methods describe the optical response in terms of global (many-electron) eigenstates. It is hard to develop an intuitive physical picture in terms of these eigenstates. To illustrate this, let us examine the two- and three-level models which are commonly used to describe the first-, second-, and third-order static response. The resulting expressions depend on a few parameters which may be computed or estimated from experimental data and provide fairly good approximations for the magnitudes of the polarizabilities. The two-level formulas for the linear (α) and quadratic (β) response are

(1) Brédas, J. L.; Adant, C.; Tackx, P.; Persoons, A. *Chem. Rev.* **1994**, *94*, 243; Bredas, J. L.; Cornill, J.; Beljonne, D.; dos Santos, D. A.; Shuai, Z. *Acc. Chem. Res.* **1999**, *32*, 267.

(2) Kanis, D. R.; Ratner, M. A.; Marks, T. J. *Chem. Rev.* **1994**, *94*, 195.

(3) Zyss, J.; Chemla, D. S., Eds.; *Nonlinear Optical Properties of Organic Molecules and Crystals*; Academic Press: Florida, 1987, Vols. 1 and 2.

(4) Bubeck, C. In *Electronic Materials: The Oligomer Approach*; Müllen, K., Ed.; John Wiley & Sons: New York, 1998.

(5) Tykewski, R. R.; Gubler, U.; Martin, R. E.; Diederich, F.; Bosshard, Ch.; Günter, P. *J. Phys. Chem. B* **1998**, *102*, 4451; Martin, R. E.; Diederich, F. *Angew. Chem.* **1999**, *38*, 1350.

(6) Zhao, M.-T.; Singh, B. P.; Prasad, P. N. *J. Chem. Phys.* **1988**, *89*, 5535.

(7) Thienpont, H.; Rikken, G. L. J. A.; Meijer, E. W.; ten Hoeve, W.; Wynberg, H. *Phys. Rev. Lett.* **1990**, *65*, 2141.

(8) Morley, J. O. *J. Chem. Soc., Faraday Trans.* **1991**, *87*, 3009.

(9) Beljonne, D.; Shuai, Z.; Brédas, J. L. *Int. J. Quantum Chem.* **1994**, *52*, 39.

(10) Tretiak, S.; Chernyak, V.; Mukamel, S. *Chem. Phys. Lett.* **1998**, *287*, 75; Tretiak, S.; Chernyak, V.; Mukamel, S. *Chem. Phys. Lett.* **1999**, *245*, 145.

(11) Samuel, I. D. W.; Ledoux, I.; Dhenaut, Ch.; Zyss, J.; Fox, H. H.; Schrock, R. R.; Silbey, R. J. *Science (Washington, D.C.)* **1994**, *265*, 1070; Delporte, C.; Ledoux, I.; Samuel, I. D. W.; Zyss, J.; Yaliraki, S. N.; Fox, H. H.; Schrock, R. R.; Silbey, R. J. *Chem. Phys.* **1999**, *245*, 1.

(12) Chernyak, V.; Mukamel, S. *J. Chem. Phys.* **1996**, *104*, 444; Tretiak, S.; Chernyak, V.; Mukamel, S. *Int. J. Quantum Chem.* **1998**, *70*, 711.

(13) Tretiak, S.; Chernyak, V.; Mukamel, S. *Chem. Phys. Lett.* **1996**, *259*, 55; Tretiak, S.; Chernyak, V.; Mukamel, S. *J. Chem. Phys.* **1996**, *105*, 8914; Tretiak, S.; Chernyak, V.; Mukamel, S. *Phys. Rev. Lett.* **1996**, *77*, 4656.

(14) Ward, J. F. *Rev. Mod. Phys.* **1965**, *37*, 1.

(15) Orr, B. J.; Ward, J. F. *Mol. Phys.* **1971**, *20*, 513.

(16) Heflin, J. F.; Wong, K. Y.; Zamani-Khamini, Q.; Garito, A. F. *Phys. Rev. B: Condens. Matter* **1988**, *38*, 1573.

(17) Rodenberger, D. C.; Heflin, J. F.; Garito, A. F. *Nature (London)* **1992**, *359*, 309.

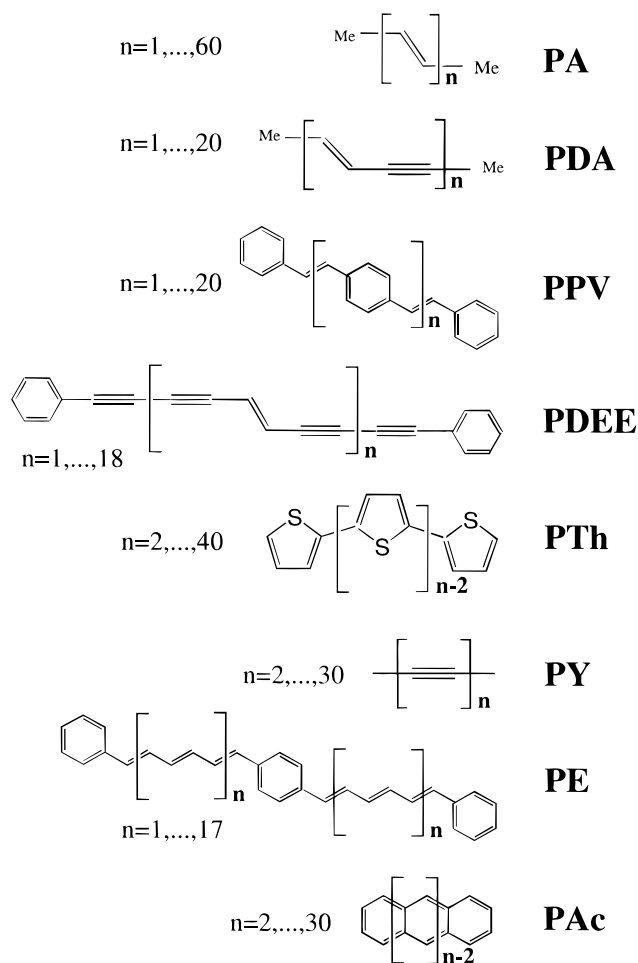


Figure 1. Chemical structures of the oligomers studied; the variation of the number of repeat units n considered in this article is indicated.

$$\alpha \propto \frac{\mu_{ge}^2}{E_{ge}} \quad (1.1)$$

$$\beta \propto (\mu_{ee} - \mu_{gg}) \frac{\mu_{ge}^2}{E_{ge}^2} \quad (1.2)$$

Here μ_{gg} and μ_{ee} are the ground- and excited-state dipole moments, μ_{ge} is the transition dipole, and E_{ge} is the electronic-transition frequency. The third-order polarizability is similarly represented by the three-level expression

$$\gamma \propto \frac{\mu_{ge_1}^2 \mu_{e_1 e_2}^2}{E_{ge_1}^2 E_{e_1 e_2}} - \frac{\mu_{ge_1}^4}{E_{ge_1}^3} + \frac{\mu_{ge_1}^2 (\mu_{e_1 e_1} - \mu_{gg})^2}{E_{ge_1}^3} \quad (1.3)$$

where e_1 and e_2 denote the two excited states, μ_{ge_1} and $\mu_{e_1 e_2}$ are the transition dipoles, and E_{ge_1} , E_{ge_2} , $E_{e_1 e_2}$ are the transition frequencies.

It is not obvious how to predict the scaling of the polarizabilities with molecular size by using these expressions. Since excited states are delocalized, we can argue that $\mu_{ge}^2 \sim n$ for large n . μ_{gg} , μ_{ee} , and E_{ge} should saturate (i.e., become size-independent) with molecular size. This results in linear dependence $\alpha \sim n$ (bulk regime). At first glance, we expect linear scaling of the second-order polarizability $\beta \sim n$ as well. However, our recent studies of donor/acceptor substituted molecules using the CEO technique showed that the donor and

acceptor only affect finite regions at the molecular chain ends.¹⁰ Consequently, β (rather than β/n) saturates and becomes size-independent. The situation is even worse for the third-order response where each term in eq 1.3 scales as $\sim n^2$. It is hard to rationalize how cancellations among different contributions result in a $\gamma \sim n$ scaling as was predicted¹³ and observed.^{7,11,18} This built-in size inconsistency of the SOS approach makes it difficult to gain physical insight into the nature of the optical response and the saturation mechanisms of electronic polarizabilities.

The synthesis of new optical materials for technological applications requires a good physical intuition about the mechanisms that control the molecular optical response to an external field. The many-electron wave function is, however, too complex, contains too much information, and is therefore unlikely to provide physical insight into the structure–function relationships. It is therefore desirable to adopt an alternative real-space picture of the optical response which should clearly show the relation between electronic motions induced upon optical excitation and the structural features of the molecule. Such a picture is provided by the CEO approach, which lends itself readily to the interpretation of the time-dependent optical response. In this picture, we describe the electronic motions using collective variables which represent the single electron density matrix and behave as classical oscillators. The method has been previously applied to several conjugated molecules. In this paper, we report a systematic study of α and γ for eight families of oligomers. In section 2 we review the main ideas of the CEO representation. The calculations are then presented in section 3, followed by a discussion and a summary in section 4.

2. The CEO Picture

Our real-space analysis of the optical response is based on the reduced single-electron density matrix, which is related to the time-dependent wavefunction of the optically driven molecule $\Psi(t)$ by

$$\rho_{mn} = \langle \Psi(t) | c_n^\dagger c_m | \Psi(t) \rangle \quad (2.1)$$

where c_n^\dagger and c_n are the creation and annihilation operators, respectively, of an electron in the n th atomic orbital (AO). The density matrix elements are thus directly associated with distinct positions of electrons and holes in real space.

The time-dependent density matrix of a molecule driven by a weak external optical field can be decomposed into a ground-state contribution $\bar{\rho}$ and a field-induced time-dependent part, i.e.

$$\rho_{mn}(t) = \bar{\rho}_{mn} + \delta\rho_{mn}^{(1)}(t) + \delta\rho_{mn}^{(2)}(t) + \delta\rho_{mn}^{(3)}(t) + \dots \quad (2.2)$$

where $\delta\rho_{mn}^{(k)}(t)$ denotes the k th order contribution in the external field. The diagonal elements $\delta\rho_{mm}^{(k)}$ represent the charge densities induced at the m th AO by the external field, whereas the off-diagonal elements $\delta\rho_{mn}^{(k)}$ with $m \neq n$ reflect the optically induced coherence between the m th and n th AO, which represents the probability to find an electron–hole pair in which the electron (hole) is located at the m th (n th) AO. The density matrix thus provides a real-space picture of the optical response, order by order, in the driving field.

The polarization can be expressed in terms of the density matrix

$$P^{(k)} = \sum_{nm} \mu_{nm} \delta \rho_{mn}^k \quad (2.3)$$

where $\mu_{mn} = \langle m | \mu_z | n \rangle$ and μ_z is the dipole operator along the molecular z axis. The polarizabilities α, β and γ are related to $P^{(1)}, P^{(2)}$, and $P^{(3)}$, respectively. The linear polarizability $\alpha(\omega)$, for example, is given by

$$\alpha(\omega) = \sum_{\nu} \sum_{mnl} \mu_{mn} \mu_{kl} \frac{2\Omega_{\nu}(\xi_{\nu})_{mn}(\xi_{\nu})_{kl}}{\Omega_{\nu}^2 - (\omega + i\Gamma_{\nu})^2} \equiv \sum_{\nu} \frac{f_{\nu}}{\Omega_{\nu}^2 - (\omega + i\Gamma_{\nu})^2} \quad (2.4)$$

Here $(\xi_{\nu})_{mn} = \langle \Psi_{\nu} | c_m^{\dagger} c_n | \Psi_g \rangle$ are the transition density matrixes (electronic normal modes) where Ψ_g and Ψ_{ν} denote the many-electron ground state and the ν th excited state, respectively. $\Omega_{\nu} = E_{\nu} - E_g$ denotes the transition frequency between the ground and an excited state, Γ_{ν} represents the dephasing rate, and the definition of the oscillator strengths f_{ν} follows from comparing the last two expressions for α . Typically $\Gamma_{\nu} \ll \Omega_{\nu}$, and in the static ($\omega \rightarrow 0$) limit this simplifies to

$$\alpha(0) = \sum_{\nu} \frac{f_{\nu}}{\Omega_{\nu}^2} \quad (2.5)$$

In an analogous way, the third-order nonlinear polarizability γ can be expressed in terms of frequencies and oscillator strengths.^{13,19}

The CEO method was first formulated in connection with the Pariser–Parr–Pople (PPP) Hamiltonian and applied to the calculation of the linear and nonlinear optical response of neutral polyenes (up to 80 carbon atoms).²⁰ Tretiak et al. employed the CEO approach combined with the PPP Hamiltonian to calculate the first-, third- and fifth-order polarizability of polyenes with as many as 200 carbon atoms.¹³ In a subsequent study,¹⁹ the semiempirical INDO/S Hamiltonian was used to compute the first-, second- and third-order polarizability of neutral as well as donor and/or acceptor substituted polyenes with chain lengths of as great as 80 carbon atoms. Origin, scaling, and saturation of the second-order polarizabilities in donor/acceptor polyenes have been explored.^{10,21} Geskin and Brédas²² investigated the third-order polarizability of polyenes with as many as 80 carbon atoms on the basis of a local analysis of atomic p-orbital electric-field-induced polarization. A CEO investigation using the PPP Hamiltonian of PPV oligomers with as many as 50 repeat units has been conducted by Mukamel et al.²³

A notable advantage of the CEO approach is that the calculation of the many-electron wave functions, which carry much more information than is needed, is entirely circumvented. Instead, the reduced description of the optical response contained in the matrixes ξ_{ν} can be obtained directly by calculating these matrixes and the corresponding frequencies Ω_{ν} by solving the time-dependent Hartree–Fock (TDHF) equations.^{12,19} Computation time only scales as $\sim N^3$ (N being the basis set size) as opposed to N^7 .^{13,19} In practice, only a few electronic modes

contribute to the optical response, which reduces the computational cost even further. In the calculations presented in this article, e.g., we found it sufficient to compute only 12 modes for the first-order optical response and 11 modes for the third-order response for all of the larger oligomers. For some of the smaller oligomers, we included one additional mode, but with no significant effect on the results. The small number of significant modes in the CEO picture further provides an intuitively appealing physical interpretation of the optical response. This is analogous to the state of affairs in infrared and Raman spectra which are typically dominated by a few active nuclear normal modes.

3. Size-Scaling of Optical Polarizabilities

Theoretical and experimental studies of the optical properties of polymers with varying chain lengths have been conducted by several authors. Hurst et al.²⁴ calculated α and γ for polyenes with 4–22 carbon atoms using the coupled/perturbed Hartree–Fock theory. Kirtman et al.²⁵ reported ab initio restricted Hartree–Fock calculations of α and γ on polyenes varying from 4 to 44 carbon atoms. Another ab initio Hartree–Fock study has been conducted by Lu et al.²⁶ for as many as 98 carbon atoms. Fanti and Zerbetto employed a sum over molecular orbitals scheme to study the evolution of γ in polyenes with chain length of as many as 160 carbon atoms.¹⁸ A comparison of the second-order polarizability of donor/acceptor substituted cumulenes, polyenes, and polyynes has been made by Morley²⁷ for chain lengths varying between 4 and 44 carbon atoms. That work was based on an initial-configuration interaction treatment of the ground- and excited-state wave functions followed by a calculation of the third-order polarizability tensor using a sum-over-states treatment of singly excited states. The same method was employed to study donor/acceptor substituted polythiophenes, polyfurans, and polypyrroles with 1–9 repeat units.⁸ Beljonne et al. calculated the third-order polarizability of polythiophenes and pyrrole oligomers using the sum-over-states method on the basis of intermediate neglect of differential overlap/multireference-determinant-configuration interaction calculations.⁹ The chain length was varied between 1 and 8 (thiophenes) and 1 and 7 (pyrroles). Zhao et al. conducted refractive-index measurements as well as degenerate four-wave mixing studies to determine the first- and third-order polarizability, respectively, of thiophene oligomers with 1 and 6 repeat units.⁶ Thienpont et al. further obtained the first-order polarizability of oligothiophenes from refractive-index measurements and the third-order polarizability by using electric-field-induced second-harmonic generation.⁷ They observed saturation of both quantities by varying the chain length between 3 and 11 repeat units. Lu et al. applied a valence-bond charge-transfer exciton model of polymer excited states to calculate the first- and third-order polarizabilities of oligothiophenes with as many as 15 repeat units and estimated the saturation lengths for oligothiophenes, polyacetylene, polyparaphenylene, polyparaphenylene vinylene, polypyrrole, polythiophene vinylene, polyethylene sulfide, polymethineimine, polybenzothiophene, and polydiacetylene.²⁸ A study of the third-order nonlinear optical properties of various

(19) Tretiak, S.; Chernyak, V.; Mukamel, S. *J. Am. Chem. Soc.* **1997**, *119*, 11408.

(20) Mukamel, S.; Takahashi, A.; Wang, H. X.; Chen, G. *Science* **1994**, *266*, 251.

(21) Tretiak, S.; Chernyak, V.; Mukamel, S. *Chem. Phys.* 1999, in press.

(22) Geskin, V. M.; Brédas, J. L. *J. Chem. Phys.* **1998**, *109*, 6163.

(23) Mukamel, S.; Tretiak, S.; Wagersreiter, T.; Chernyak, V. *Science* **1997**, *277*, 781.

(24) Hurst, G. J. B.; Dupuis, M.; Clementi, E. *J. Chem. Phys.* **1988**, *89*, 385.

(25) Kirtman, B.; Toto, J. L.; Robins, K. A.; Hasan, M. *J. Chem. Phys.* **1995**, *102*, 5350.

(26) Lu, D.; Marten, B.; Ringnalda, M.; Friesner, R. A.; Goddard, W. A., III. *Chem. Phys. Lett.* **1996**, *257*, 224.

(27) Morley, J. O. *J. Phys. Chem.* **1995**, *99*, 10166.

(28) Lu, D.; Chen, G.; Goddard, W. A., III. *J. Chem. Phys.* **1994**, *101*, 4920.

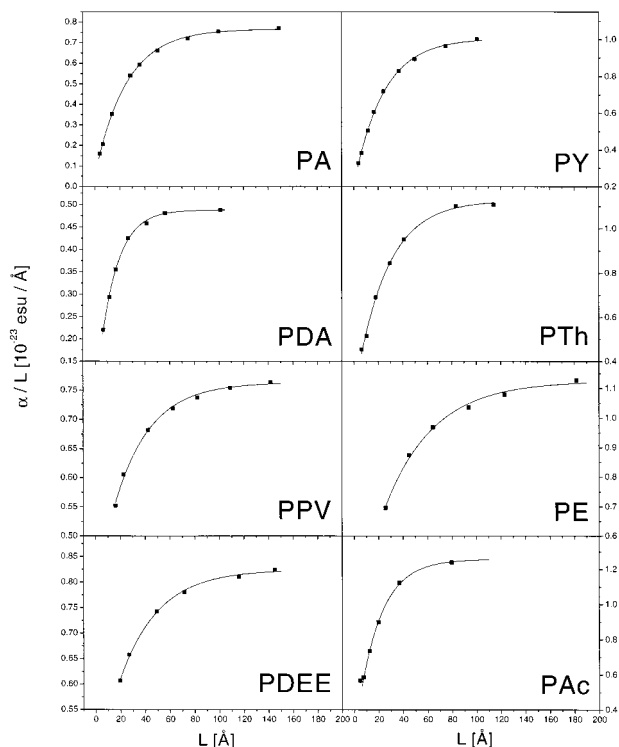


Figure 2. First-order optical polarizability per molecular chain length α/L in units of 10^{-23} esu/Å vs chain length L in units of Ångströms. The computed values are indicated by squares, the fitting results according to eq 3.1 are represented by a solid line.

1,2 diethynylethene and tetraethynylethene oligomers can be found in a recent paper by Tykwinski et al.⁵

We have computed the first- and third-order off-resonance optical response and its chain-length dependence for polyacetylenes (PA), polydiacetylenes (PDA), poly (*p*-phenylene vinylene) (PPV), poly (1,2 diethynylethenes) (PDEE), polythiophenes (PTh), polyynes (PY), and polyacenes (PAc), as well as for a polyenic molecule similar to one investigated experimentally by Samuel et al.¹¹ (abbreviated here by PE).

The molecules and the range of the number of repeat units n considered in this study are shown in Figure 1. Molecular geometries have been optimized with the GAUSSIAN 94 package at the AM1 level. We subsequently used the ZINDO program to build the INDO/S Hamiltonian.^{29–31} The ground-state density matrix $\bar{\rho}$ has been computed by solving the Hartree-Fock equation self-consistently, using the INDO/S Hamiltonian. The CEO which employs the density-matrix spectral moment algorithm (DSMA) has been used.¹⁹ The ground-state density matrix was used as an input to the DSMA, which yielded the first- and the third-order density matrix response $\delta\rho^{(1)}$ and $\delta\rho^{(3)}$ and the corresponding off-resonant optical polarizabilities, α and γ . By considering the polarizabilities of the eight different classes of oligomers in the zero-frequency limit, we can directly compare their scaling with chain length without having to worry about possible resonance enhancements which occur at different frequencies for different oligomers and complicate the analysis.

Figures 2 and 3 show the first- and the third-order polarizability per unit length, α/L and γ/L , respectively, as a function of chain length L . The calculated values are represented by solid squares. For all families of oligomers, α/L initially increases

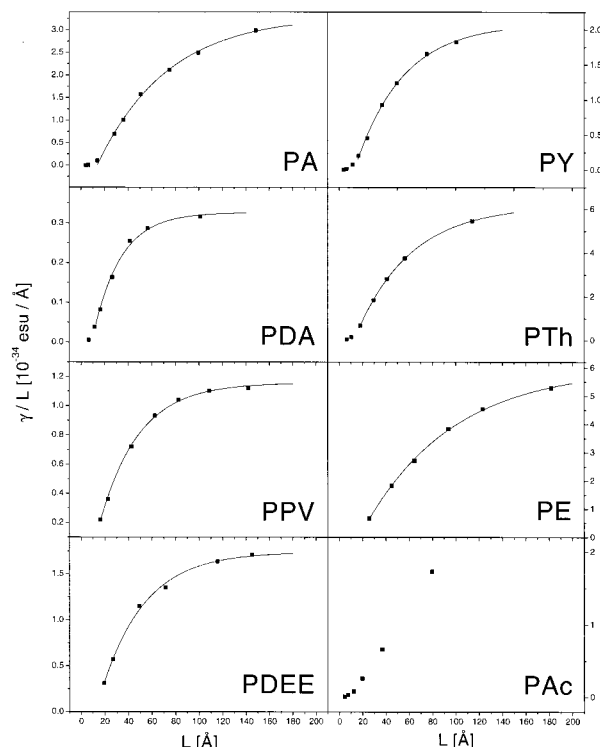


Figure 3. Third-order optical polarizability per molecular chain length γ/L in units of 10^{-34} esu/Å vs chain length L in units of Ångströms. The computed values are indicated by squares, the fitting results according to eq 3.1 are represented by a solid line.

with L and then reaches a plateau, indicating that α becomes an extensive quantity. The behavior of γ is very similar. However, in all families studied, the saturation of γ occurs at a much higher chain length compared with that of α . No saturation of γ/L could be observed for Polyacenes within the range of chain lengths studied (80 Å or 30 repeat units). For larger Polyacene oligomers, the GAUSSIAN 94 geometry optimization at the AM1 level did not converge.

The variation in the characteristic saturation chain length can be quantified by a suitable fit of the polarizability curves in Figures 2 and 3. In earlier studies, the variation of the polarizability χ (where $\chi = \alpha, \gamma$) with the number of repeat units n has been described by a power law n^b .^{13,20} However, since the scaling exponent b varies strongly with n , the power law does not provide a concise characterization of the saturation curves of χ in terms of a few parameters. Rather, it merely replaces the description of the saturation behavior in terms of the function $\chi(n)$ with the new function $b(n)$. Instead, we found that the expression

$$\chi(L)/L = D - C \exp(-L/L_s) \quad (3.1)$$

gives very good fits, as shown by the solid lines in Figures 2 and 3. The parameter L_s provides a measure for the characteristic saturation length of each family of oligomers. It represents the chain length at which the polarizability has reached its asymptotic value within $1/e$. The parameters C , D , and L_s are listed in Table 1 for all eight families of oligomers (superscripts (1) and (3) denote parameters of α and γ , respectively). The number of repeat units, n_s , and the total number of heavy atoms in the molecule, N_s , corresponding to the saturation length L_s are given as well. No parameters are presented for Polyacenes in third order, since saturation has not been obtained in the size range studied. We note that D gives the asymptotic value of α/L and

(29) Pople, J. A.; Segal, G. A. *J. Chem. Phys.* **1965**, *43*, S136.

(30) Ridley, J.; Zerner, M. C. *Theor. Chim. Acta* **1973**, *32*, 111.

(31) Zerner, M. C.; Loew, G. H.; Kirchner, R. F.; Mueller-Westerhoff, U. T. *J. Am. Chem. Soc.* **1980**, *102*, 589.

Table 1. Fitting Parameters L_s , C , and D of the Linear (α) and Third-Order (γ) Polarizabilities (See Equation 3.1)

oligomer family	$L_s^{(1)}$ [Å]	$n_s^{(1)b}$	$N_s^{(1)}$	$L_s^{(3)}$ [Å]	$n_s^{(3)}$	$N_s^{(3)}$	A^a [Å] B [Å]
	$C^{(1)}$ [10^{-23} esu/Å]			$D^{(1)}$ [10^{-23} esu/Å]			
polyacetylene (PA)	25.34	9.8	21.6	59.39	23.7	49.3	−1.081 1.226
	0.709			4.176			
	0.766			3.313			
polydiacetylene (PDA)	14.23	2.6	12.2	23.26	4.4	19.5	−0.971 1.243
	0.424			0.482			
	0.488			0.326			
poly(<i>p</i> -phenylene vinylene) (PPV)	28.63	2.9	37.3	32.93	3.6	42.5	−2.197 0.827
	0.340			1.547			
	0.743			1.157			
poly(diethylethene) (PDEE)	31.04	2.6	31.4	36.08	3.3	35.5	−7.601 1.231
	0.402			2.442			
	0.824			1.738			
polythiophene (PTh)	25.79	7.1	35.3	47.08	12.6	62.9	−1.389 0.770
	0.879			8.040			
	1.128			6.175			
polyyne (PY)	24.24	10.1	22.1	41.03	16.6	35.2	−3.898 1.275
	0.795			2.857			
	1.004			2.087			
polyethylenic oligomer (PE)	39.92	2.5	41.9	77.11	6.3	72.3	−11.125 1.220
	0.803			7.475			
	1.125			6.017			
polyacene (PAc)	18.79	7.5	39.9				−7.952 0.670
	0.996						
	1.258						

^a Parameters A and B represent the linear relation between chain length and number of atoms in the polymer (see eq 3.2). ^b n_s and N_s are the number of repeat units and the total number of heavy atoms, respectively, corresponding to L_s .

γ/L . The table also provides the parameters A and B of the linear relation

$$L(N_0) = A + BN_0 \quad (3.2)$$

between the chain length L and the number N_0 of heavy atoms of the oligomer.

We note that our result for the asymptotic value of α/L for PA is $D^{(1)} = 0.77 \times 10^{-23}$ esu/Å, which compares reasonably well with that reported by Kirtman et al.²⁵ of 0.82×10^{-23} esu/Å for a polyenic chain of 44 carbon atoms, where we have converted the results reported in that article into our units. Lu et al. reported an asymptotic value of 0.92×10^{-23} esu/Å. Our asymptotic value for $\gamma/L = 3.31 \times 10^{-34}$ esu/Å lies between the result of Lu et al. (1.55×10^{-34} esu/Å) and that of Kirtman et al. (6.32×10^{-34} esu/Å).

4. Discussion

Our modeling results for the various classes of oligomers allow us to make a number of interesting comparisons. Both the PA and the PE oligomers, e.g., have a polyene-like backbone. We can see in Table 1 that the saturation length of PA involves approximately four times as many repeat units compared with that of PE. However, we can see from Figure 1 that this saturation length corresponds to exactly the same number of double bonds for both classes of oligomers. This suggests that the central phenyl ring in the PE oligomers which connects the two polyene segments through the para position does not break the conjugation. A similar observation is made for the third-order saturation length. However, remarkably enough, the asymptotic value D of α/L and γ/L for the PE oligomers is almost twice as high as compared with that of the PA oligomers, namely (in 10^{-23} esu/Å), 1.13 for PE as compared with 0.77 for PA, for the first-order response, and (in 10^{-34} esu/Å) 6.02 for PE as compared with 3.31 for PA for the third-order response.

More interesting observations can be made by comparing the results for the PA oligomers consisting of a polyenic chain and PY oligomers consisting of a polyynic chain with the PDA oligomer, which is a combination of double and triple bonds. We can see in Table 1 that the saturation lengths $n_s^{(1)}$ are comparable for PA and PY, whereas PY has a somewhat higher saturation value of $\alpha/L = D^{(1)} = 1.00$ as compared with 0.77 for PA (in 10^{-23} esu/Å). However, the combination of double and triple bonds in PDA results in a saturation length n_s that is only 1/4 of the corresponding value for PA and PY. Given that one PDA repeat unit contains twice as many heavy atoms as one PA or PY repeat unit (see Figure 1), we still see that saturation occurs in PDA at a chain length containing only half as many heavy atoms compared with the corresponding saturation length in PA and PY. Moreover, the asymptotic value of $\alpha/L = 0.49$ in PDA is clearly smaller than in PA and PY. Similar effects are observed by comparing the calculations for the third-order optical response. This suggests that the combination of double and triple bonds in PDA restricts the freedom of the electron–hole pairs to respond to the external electromagnetic field, resulting in a shorter saturation size and a smaller asymptotic value of α/L and γ/L .

The comparison of PA and PY with PDEE, which also combines double and triple bonds, is somewhat less dramatic. The saturation size $n_s^{(1)}$ of PDEE is again 1/4 of the corresponding value of PA and PY. However, since PDEE contains three times as many heavy atoms per repeat unit compared with PA and PY, this only means that saturation occurs at a chain length containing approximately 3/4 as many heavy atoms as compared with the saturation chain length of PA and PY. The fact that $L_s^{(1)}$ is even larger for PDEE than for PA and PY is due to the additional length of the end units of PDEE. In contrast to PDA, which contains as many double as triple bonds, we observe in PDEE, which contains twice as many triple bonds as double bonds per repeat unit, an asymptotic value of α/L which lies between the corresponding values for PA and PY, namely, $\alpha/L = 0.82$. This suggests that the electron–hole pairs

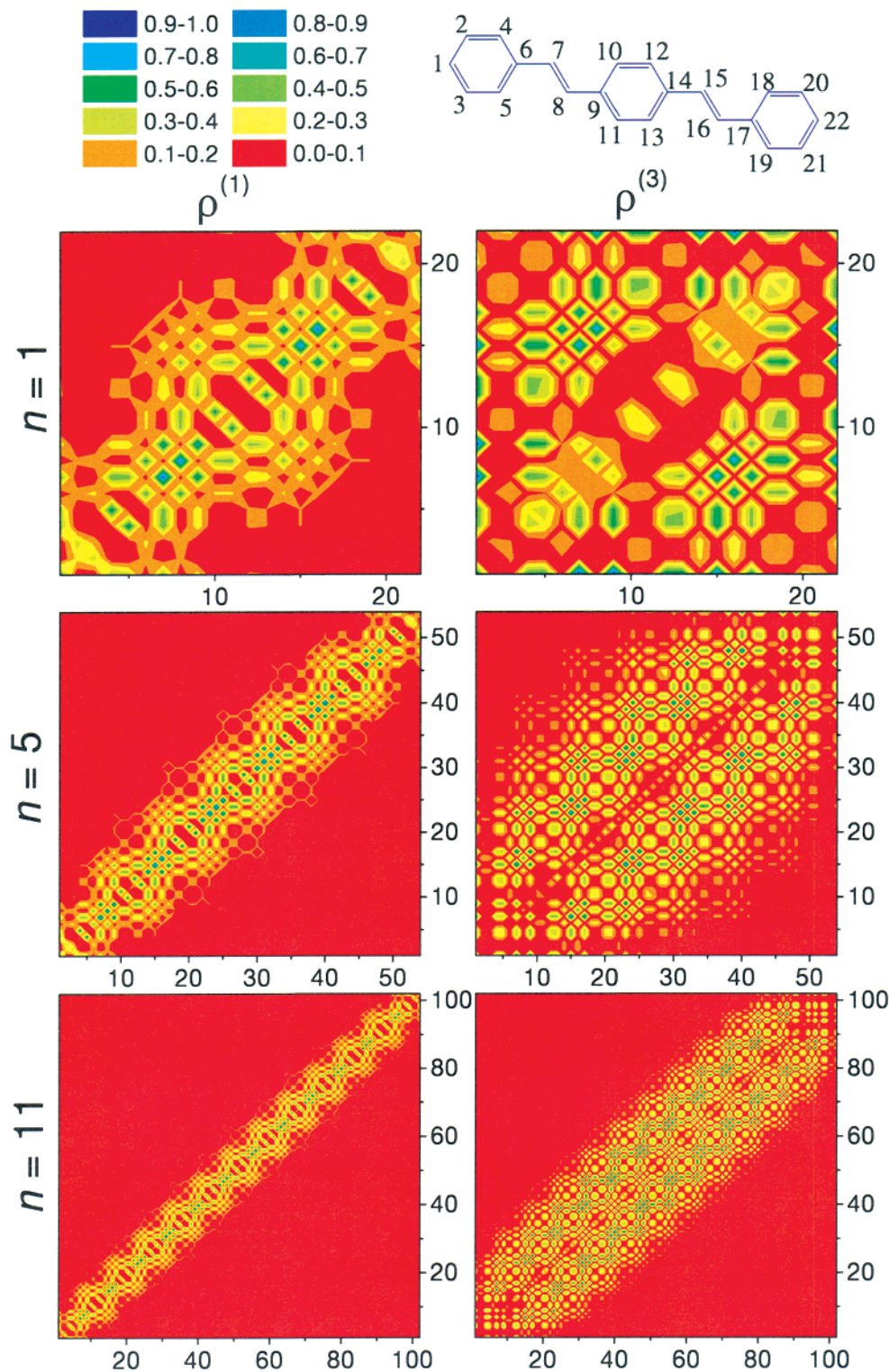


Figure 4. Contour plots of the first-order (left column) and third-order (right column) off-resonance density matrix response of a PPV oligomer with 1 (top row), 5 (middle row), and 11 (bottom row) repeat units. The axes label the atoms according to the labeling convention indicated above in a PPV molecule with one repeat unit.

have a larger freedom to move in first-order response to an external electromagnetic field as compared with PDA. For the third-order response, we observe that the asymptotic value of γ/L for PDEE is smaller than the same value for PA and PY, but again considerably larger than the one for PDA.

A comparison of the results for PPV and PAc offers more interesting observations. Even though the saturation length for PAc ($n_s = 7.5$, corresponding to approximately 30 heavy atoms in the repeat units) is somewhat larger than the saturation length

for PPV ($n_s = 2.9$, corresponding to approximately 23 heavy atoms in the repeat units), the saturation length of the entire molecule L_s (in Å) is smaller for PAc than for PPV, since the molecular structure is more “compact”. The asymptotic value of α/L for PAc (1.26) is considerably larger than the corresponding value for PPV (0.74).

We can rationalize our results for the saturation behavior of the different classes of organic oligomers by examining the first and the third order optically induced density matrix response.

Figure 4 shows contour plots for PPV of $\delta\rho^{(1)}$ (left column) and $\delta\rho^{(3)}$ (right column), with $n = 1$ (top row), $n = 5$ (middle row), and $n = 11$ (bottom row) repeat units. The numbering convention of atoms in the PPV molecule is shown for one repeat unit. The abscissa and ordinate in Figure 4 represent the electron and the hole coordinate, respectively. The magnitude of the element $\rho_{mn}^{(k)}$ represents the probability of finding an electron-hole pair (exciton), induced by the external field in k th order, with the electron and the hole centered at the m th and the n th carbon atom, respectively. Our convention for the depiction of the density matrix is such that the element $\delta\rho_{11}^{(k)}$ is located in the bottom left corner of each contour plot, and the diagonal of the matrix runs from the bottom left to the top right corner. The plots clearly show that the collective electronic motions are delocalized across the entire molecule. The exciton radius (or coherence size) is given by the antidiagonal size of the density matrix. The phenyl rings are clearly distinguishable, particularly in the plots of $\delta\rho^{(1)}$, since the coherence size is larger in the phenyl rings than in the vinyl bridges. $\delta\rho^{(3)}$ shows a large coherence between first and second nearest neighbor phenyl rings, whereas the coherence in $\delta\rho^{(1)}$ only extends to atoms within the same phenyl ring. An analogous observation holds for the atoms in the vinyl bridges. The plots of $\delta\rho^{(1)}$ and $\delta\rho^{(3)}$ for the other families of oligomers (not shown) look very similar.

The real-space picture of the optical response pinpoints the physical origin of the saturation behavior of optical polarizabilities.¹⁰ For short chain lengths, the excitons' natural radii are larger than the molecular size. Thus, an increase in chain length results in more freedom for the electrons and holes to move in response to the driving field and, consequently, in higher polarizabilities. However, once the chain length becomes large in comparison with the exciton radius, a further increase in chain length does not affect the mobility of the charges set in motion by the external field and thus has no further effect on the polarizability. (We note that we use different axis scales in Figure 4. Once the size of the molecule becomes larger than the exciton radius, the antidiagonal size of the density matrix does not increase any further with increasing n). This is a similar picture to quantum confinement in semiconductor nanoparticles.^{32–34} However, the present excitons are charge-transfer rather than Wannier type. The larger coherence size observed in the third-order response as compared with the first-order response clearly explains why the saturation size L_s is larger for γ than for α .

To quantify this qualitative interpretation of the size scaling of the off-resonance polarizabilities, we introduce a characteristic coherence size $L_\rho^{(k)}$ of the k th order density matrix response, defined as the inverse participation ratio:^{35,36}

$$L_\rho^{(k)} = [N_0 \sum_{m,n} |\rho_{mn}^{(k)}|^2]^{-1} [(\sum_{m,n} |\rho_{mn}^{(k)}|)^2] \quad (4.1)$$

$L_\rho^{(k)}$ provides a measure for the characteristic length scale of $\delta\rho^{(k)}$ along the antidiagonal direction. For a localized response in the absence of coherence, $\rho_{nm} = \delta_{nm}/N_0$ and thus $L_\rho = 1$. For a completely delocalized response, we have $\rho_{nm} = 1/N_0$ and $L_\rho = N_0$, which corresponds to maximum coherence. To compare the saturation size L_s with this quantity, we recall that

(32) Haug, H.; Koch, S. W. *Quantum Chemistry of the Optical and Electronic Properties of Semiconductors*; World Scientific: Singapore, 1990.

(33) Nirmal, M.; Norris, D. J.; Kuno, M.; Bawendi, M. G.; Efros, A. L.; Rosen, M. *Phys. Rev. Lett.* **1995**, *75*, 3728.

(34) Alivisatos, A. P. *Science (Washington, D.C.)* **1996**, *271*, 993.

(35) Meier, T.; Zhao, Y.; Chernyak, V.; Mukamel, S. *J. Chem. Phys.* **1997**, *107*, 3876.

(36) Economou, E. N. *Green's Functions in Quantum Physics*; Springer: New York, 1983.

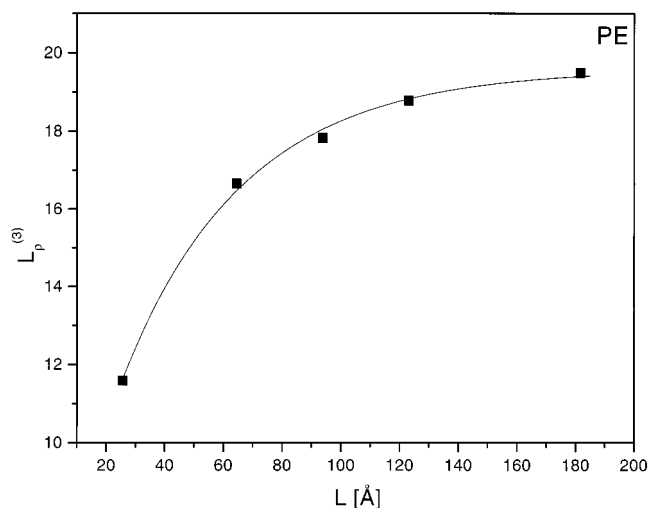


Figure 5. Inverse participation ratio (unitless) vs chain length (in Ångströms) for the third-order optical response of the PE oligomers. The computed values are indicated by squares; the fitting results are represented by a solid line.

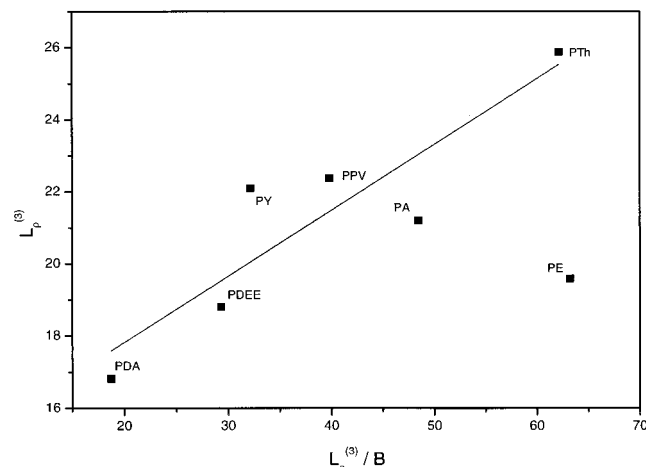
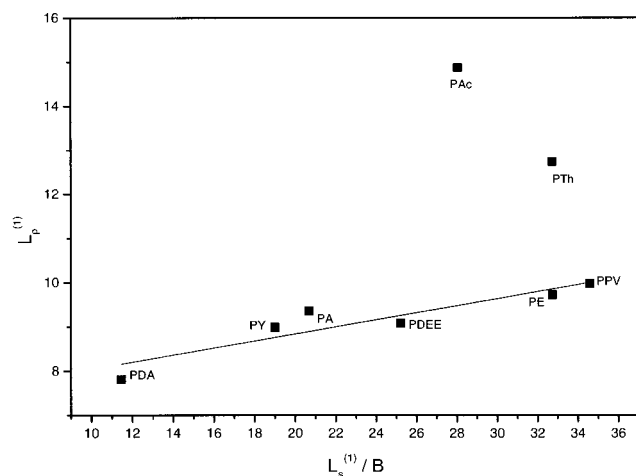


Figure 6. Inverse participation ratio (unitless) vs saturation size L_s/B (unitless) for the first- (top) and third- (bottom) order optical response. The computed values are indicated by squares; the linear fit is represented by a solid line.

L_s is in units of Ångströms, whereas $L_\rho^{(k)}$ is dimensionless, given in units of atom labels. We therefore divide L_s by the parameter B (see eq 3.2). It should be pointed out that $L_\rho^{(k)}$, computed for a given family of oligomers, also depends on chain length, as can be seen in Figure 5 for PE. The solid squares represent

$L_\rho^{(3)}$ as a function of chain length. To obtain a meaningful measure for the characteristic coherence size of the optically induced electron–hole pairs in the molecule, $L_\rho^{(k)}$ should be computed for a large enough oligomer. Alternatively, if results are available for several chain lengths, as in Figure 5, but $L_\rho^{(k)}$ has not quite converged within the range of chain lengths considered, one can also fit $L_\rho^{(k)}$ vs L by employing the same expression used to fit χ/L vs L , eq 3.1. The result of this fit is represented in Figure 5 by the solid line. D then provides an extrapolated value of $L_\rho^{(k)}$ for $L \rightarrow \infty$. Figure 6 shows $L_\rho^{(k)}$ vs $L_s^{(k)}/B$, where $k = 1$ (top) and $k = 3$ (bottom). Each point represents a different class of oligomers, as indicated. Most oligomers considered show a linear relation between the coherence size of the optical response, given by the inverse participation ratio $L_\rho^{(k)}$, and the saturation size of the first- and third-order polarizabilities α and γ , represented by $L_s^{(1)}$ and $L_s^{(3)}$, respectively. This analysis shows a strong correlation between the optical coherence and the oligomeric chain-size saturation of the optical polarizabilities, as suggested by a qualitative comparison of Figure 4 with Figures 2 and 3. Some oligomers do not fit into the same linear relation. We expect that other families of oligomers may show a linear relation between $L_\rho^{(k)}$ and $L_s^{(k)}/B$, but with a different slope than observed here.

In summary, we have investigated the first- and third-order polarizability, α and γ , of several organic oligomers and their dependence on chain length L with the CEO method. We focused on the purely electronic contribution to the polarization in this article. The role of vibrational contributions has been

discussed extensively³⁷ and goes beyond the scope of this article. An exponential expression for α/L and γ/L as functions of L provides an excellent fit. In contrast to the conventional power law fit, this expression allows us to concisely characterize these functions in terms of three parameters that are independent of L over the entire range of chain lengths. In particular, we obtain a characteristic saturation size L_s for each family of oligomers, which describes how rapidly α/L and γ/L saturate with increasing L . A qualitative comparison with contour plots of the first- and third-order density matrix response with the saturation size suggested a correspondence between L_s and the antidiagonal size of the density matrix response, which can be interpreted as the characteristic exciton size. This implies that the saturation behavior of the polarizability of a class of oligomers can be explained in terms of the motion of excitons in real space. In particular, the polarizability saturates when the size of the oligomer is large compared with the exciton radius. We tested this qualitative picture further by describing the antidiagonal size of the density matrix response using the inverse participation ratio, L_ρ , and found that for most oligomers L_ρ varies linearly with L_s .

Acknowledgment. The support of the Air Force Office of Scientific Research Grant no. AFRSOR-F49620-96-1-0030 and the National Science Foundation through Grants nos. CHE-9526125 and PHY94-15583 is gratefully acknowledged.

JA991074H

(37) Bishop, D. M. *Adv. Chem. Phys.* **1998**, *104*, 1.